nature biotechnology

Synthetic protein scaffolds provide modular control over metabolic flux

John E Dueber[1,2], Gabriel C Wu[1,2], G Reza Malmirchegini[1,9], Tae Seok Moon[3,4], Christopher J Petzold[5,6], Adeeti V Ullal[7], Kristala L J Prather[3,4] & Jay D Keasling[1,2,5–8]

Engineered metabolic pathways constructed from enzymes heterologous to the production host often suffer from flux imbalances, as they typically lack the regulatory mechanisms characteristic of natural metabolism. In an attempt to increase the effective concentration of each component of a pathway of interest, we built synthetic protein scaffolds that spatially recruit metabolic enzymes in a designable manner. Scaffolds bearing interaction domains from metazoan signaling proteins specifically accrue pathway enzymes tagged with their cognate peptide ligands. The natural modularity of these domains enabled us to optimize the stoichiometry of three mevalonate biosynthetic enzymes recruited to a synthetic complex and thereby achieve 77-fold improvement in product titer with low enzyme expression and reduced metabolic load. One of the same scaffolds was used to triple the yield of glucaric acid, despite high titers (0.5 g/l) without the synthetic complex. These strategies should prove generalizeable to other metabolic pathways and programmable for fine-tuning pathway flux.

Metabolic engineering has become an attractive alternative to chemical synthesis, especially for providing a means to generate fuels from renewable resources[1], convert biomass into both bulk and specialty chemicals[2], and produce therapeutically relevant products[3] when their chemical synthesis in an environmentally friendly manner is challenging. Achieving high product titers requires that the fluxes of each enzymatic reaction of the pathway are balanced to limit the accumulation of intermediates, especially intermediates toxic to the production host. Thus, overall flux must be high without introducing excessive energy requirements.

Whereas tight regulation (e.g., positive or negative feedback) is a hallmark of natural metabolism, where 'just enough' synthesis usually provides maximum evolutionary fitness, metabolic engineers strive to maximize titers. As a consequence, expression levels of the enzymes are frequently dramatically higher in an engineered pathway than would be found in any natural metabolic pathway. The high expression levels rob the cell of nucleotides and amino acids that might have been used for biomass production or even the desired product, thereby decreasing product titers, and inducing stress responses triggered by protein overproduction[4]. Although heterologous expression may remove undesired regulatory points in natural pathways that restrict pathway flux, introduction of synthetic regulatory control for balancing the varied activity levels of the pathway enzymes is highly desirable[5–7]. Minimizing metabolite accumulation also reduces potential toxicity in heterologous production-chassis not adapted to cope with high concentrations of these compounds. However, decreasing cell-averaged intermediate concentrations to below the K_m of the enzyme that uses the metabolite can reduce pathway flux.

Two strategies for balancing pathway flux have been successfully applied: modulating the expression levels of individual enzymes (e.g., through manipulating promoter strengths, ribosome binding site strengths, plasmid copy number or tunable intergenic regions controlling mRNA processing)[8–10] and improving turnover activities of rate-limiting enzymes by directed evolution[11]. Here we describe a distinct but complementary strategy for increasing overall pathway flux while simultaneously reducing metabolic loads. Pathway enzymes are colocalized to synthetic complexes in a programmable manner using engineered interactions between well-characterized protein-protein interaction domains and their specific ligands. This increases the effective concentrations of metabolic intermediates, while preventing their accumulation to toxic levels. Moreover, varying the number of interaction domain repeats that target different enzymes to the synthetic complex can balance relative fluxes of individual enzymes to optimize production levels.

Our scaffolding strategy was inspired by natural systems exhibiting substrate channeling. Substrate channeling has several potential advantages: (i) preventing the loss of intermediates to diffusion or competing pathways, (ii) protecting unstable intermediates from solvent and/or decreasing the transit times of intermediates, and (iii) circumventing unfavorable equilibria and kinetics imposed by bulk-phase metabolite concentrations[12,13]. Tryptophan synthase and carbamoyl phosphate synthetase provide two illustrative examples of substrate channeling. The crystal structure of the tryptophan synthase

[1]California Institute of Quantitative Biomedical Research (QB3), University of California, Berkeley, California, USA. [2]Synthetic Biology Engineering Research Center (SynBERC), University of California, Berkeley, California, USA. [3]Department of Chemical Engineering, Massachusetts Institute of Technology, Cambridge, Massachusetts, USA. [4]Synthetic Biology Engineering Research Center (SynBERC), Massachusetts Institute of Technology, Cambridge, Massachusetts, USA. [5]Physical Biosciences Division, Lawrence Berkeley National Laboratory, Berkeley, California, USA. [6]Joint BioEnergy Institute, Emeryville, California, USA. [7]Department of Bioengineering, University of California, Berkeley, California, USA. [8]Department of Chemical Engineering, University of California, Berkeley, California, USA. [9]Present address: Department of Chemistry and Biochemistry, University of California, Los Angeles, California, USA. Correspondence should be addressed to J.E.D. (jdueber@berkeley.edu).

Received 10 June; accepted 7 July; published online 2 August 2009; doi:10.1038/nbt.1557

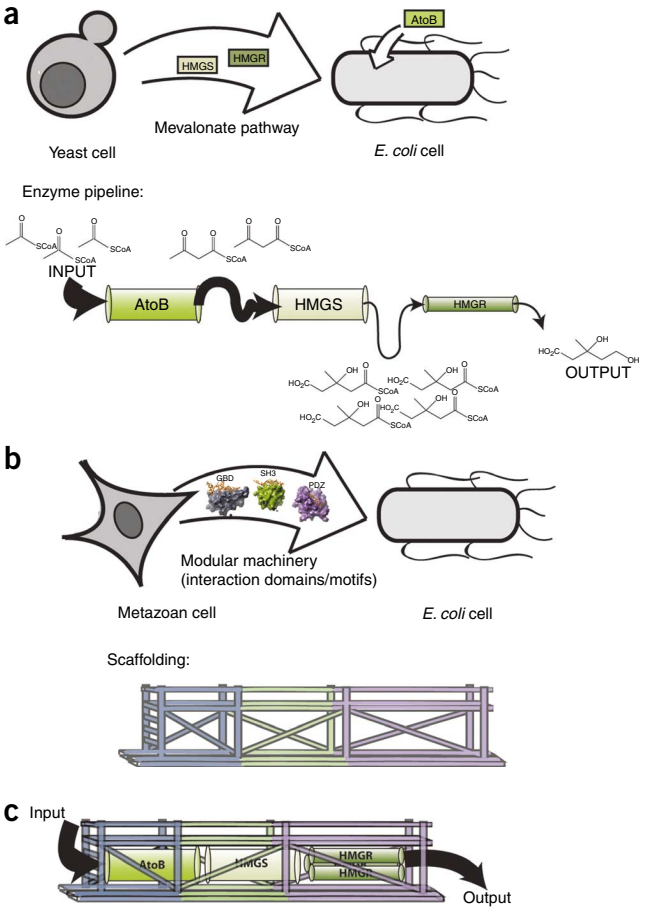

Figure 1 Employing metazoan machinery for modular control over pathway flux. (**a**) The genes encoding the mevalonate pathway enzymes (HMGS and HMGR) were taken from yeast (*S. cerevisiae*) and inserted into *E. coli* along with the *E. coli* gene encoding AtoB. These enzymes have different levels of activity, creating a bottleneck that results in accumulation of the intermediate HMG-CoA, which is toxic to *E. coli* at high concentrations[5]. Fluxes through each enzymatic step can be compared to pipes of different cross-sectional areas put together to make a pipeline. The thickness of the arrows connecting these enzymes represents the flux through these respective steps, and the resultant relative accumulation of intermediates is also depicted. (**b**) Protein-protein interaction domains and ligands from metazoan cells (mouse SH3 and PDZ domains and rat GBD) were used to design regulation machinery and inserted into these same *E. coli* cells. Thus, both the mevalonate pathway enzymes and the regulation machinery are heterologous to *E. coli*. (**c**) The scaffolded pathway is more efficient as a result of co-localizing the mevalonate enzymes to the same complex as well as optimizing the enzyme stoichiometry to balance the units of activity at the complex.

complex shows a largely hydrophobic, protected tunnel that connects active sites about 25 Å apart[14]. In addition to protection of reactive intermediates, this tunnel actively passes the indole intermediate between active sites, thereby increasing reaction kinetics. Similarly, the crystal structure of carbomoyl phosphate synthetase shows a tunnel 96 Å long, which connects three active sites[15]. Bicarbonate, glutamine and two molecules of ATP are channeled through a series of four separate reactions that produce three reactive and unstable intermediates: NH_3, carboxyphosphate and carbamate[12]. Channeling couples these required reactions at the proper stoichiometry despite a three-order-of-magnitude difference in the K_m for free NH_3 compared to that for glutamine. Polyketide synthases offer another interesting case of substrate channeling—modules comprising assembly lines of catalytic activities where substrates are directly tethered to, and processively carried through, the enzyme modules via thioester linkages. In this manner, complex small molecules can be synthesized with very low rates of loss of intermediates. These natural examples illustrate two approaches of substrate channeling: sequestration versus covalent tethering of intermediates. Instead of undertaking the difficult task of engineering protein structures that can directly replicate either of these two approaches, our scaffold design aimed to improve pathway efficiency by increasing the effective concentrations of intermediary metabolites by means of enzyme complex formation in a programmable manner.

A recent, excellent review discusses both natural substrate channeling complexes in more depth, as well as current methods and their limitations for mimicking nature's mechanisms of substrate channeling[16]. The most common technique, enzyme immobilization, suffers from the "cost associated with scale-up and cell-free systems" because these *in vitro* strategies lack the self-replicating advantages of living cells[17]. Further demand for an *in vivo* strategy comes from the successful use of crowding agents to mimic cytoplasmic conditions[18]. Fusion proteins have been used *in vivo*, but with mixed success[19]. Large fusions can impair enzyme folding, which in turn often prevents control of enzyme stoichiometry. These limitations make the use of synthetic scaffolds built from modular, genetically encoded parts an attractive alternative for reducing the apparent *in vivo* K_m for pathways that do not naturally employ complex formation. This can be achieved by relatively small modifications to the targeted enzyme in a manner that does not require structural information, similar to fusion tags added to proteins for affinity purification.

We selected the three-enzyme pathway that produces mevalonate from acetyl-CoA as a model system[20]. Mevalonate is a precursor for synthesis of the large isoprenoid family, members of which have therapeutic and commercial value[3], including the antimalarial drug artemisinin. As the mevalonate biosynthetic pathway is not endogenous to *Escherichia coli*, its heterologous expression can result in flux imbalances with high metabolic load in this production host[9]. Whereas the first enzyme in the synthetic pathway, acetoacetyl-CoA thiolase (AtoB), is native to *E. coli*, the second and third enzymes, hydroxy-methylglutaryl-CoA synthase (HMGS) and hydroxy-methylglutaryl-CoA reductase (HMGR), have been imported from *Saccharomyces cerevisiae* and codon-optimized for expression in *E. coli*. The genes encoding the pathway enzymes were placed under the heterologous transcriptional regulation of inducible promoters, and modular control was gained by using machinery evolved for signal processing in metazoan cells (**Fig. 1**). These machineries (protein-protein interaction domains and their ligands) are used in many different combinations in natural proteins to achieve different behaviors[21–23] and in synthetic proteins capable of sophisticated gating[24,25]. Thus, these domain/ligands have proven to be engineerable, as well as adaptable, and therefore provide excellent modular parts for building synthetic scaffolds. As they are not naturally present in *E. coli*, the interaction domain/ligand pairs should be programmable with minimal cross-talk with the prokaryotic cellular milieu.

RESULTS

Programmable enzyme complex formation

As a direct test of the capacity of engineered enzyme corecruitment to boost metabolite titers, we targeted the bottleneck enzymatic step of the mevalonate biosynthetic pathway (HMGR-catalyzed turnover of HMG-CoA to mevalonate) for flux improvement[9]. A synthetic complex of HMGS and HMGR was created by attaching a varying number of SH3 (Src homology 3 domain from the adaptor protein CRK)

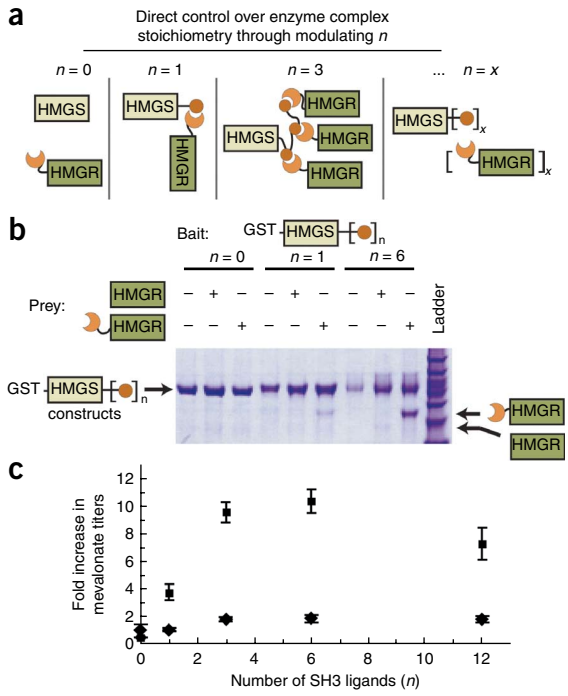

Figure 2 Heterologous protein-protein interaction domain/ligands provide direct control over enzyme stoichiometry of a synthetic complex. (**a**) A varying number of SH3 ligands were recombined to the C terminus of HMGS, and an SH3 domain was recombined to the N terminus of HMGR. (**b**) A GST pull-down was performed using HMGS bait with zero, one or six SH3 ligands and HMGR prey with and without an N-terminal SH3 domain. An interaction was observed only when both interaction partners were present and increased amounts of prey were pulled down as the number of ligands was increased. (**c**) Mevalonate production increased as the number of ligands recombined to HMGS was increased until it reached a maximum of approximately tenfold with six ligands. Improvements in mevalonate titer over that from the unscaffolded pathway decreased to approximately sevenfold when the number of ligands was further increased to 12. These significant production increases required the recombination of a corresponding SH3 domain to HMGR. Prey construct: squares, HMGR tagged with an N-terminal SH3 domain; diamonds, untagged HMGR. Error bars show 1 s.d. from an average of three separate experiments. Raw data for this experiment as well as the other mevalonate titer experiments can be found in **Supplementary Tables 2**–**7**.

interaction ligands to the C terminus of HMGS and attaching an SH3 domain to the N terminus of HMGR (**Fig. 2a**). This simple design also provided control over the relative abundances of these two enzymes in the resultant complex. The ability of these proteins to interact in an SH3-dependent manner was probed in a GST pull-down experiment (**Fig. 2b**). An N-terminal GST-tagged HMGS with zero, one or six C-terminal SH3 peptide ligands ($K_d = 0.1$ μM) was used as bait. As prey, an SH3 domain was attached to the N terminus of HMGR and its ability to bind HMGS bait was compared to HMGR alone. No significant interaction was observed between HMGS and HMGR without engineered SH3 interactions. However, HMGR with an N-terminal SH3 domain was pulled down by GST-tagged HMGS in a ligand-dependent manner. An observable amount of HMGR was pulled down when a single ligand was tethered to HMGS, but considerably more was pulled down when six ligands were tethered to HMGS. Thus, the relative stoichiometries of these two enzymes in the complex were controlled by varying the number of interaction ligands tethered to HMGS.

Improved titer production through engineered complexes

Next we tested the efficacy of improving mevalonate pathway flux *in vivo*. To maximize control over expression levels, we placed the genes encoding the first two enzymes of the pathway (AtoB and HMGS) under control of an arabinose-inducible promoter (P_{BAD}), and the gene encoding HMGR under control of a tetracycline-inducible promoter (P_{TET}) (**Supplementary Fig. 1**). All experiments were conducted with high expression levels of AtoB and HMGS, but low expression levels of the flux-limiting HMGR, to demonstrate that this bottleneck in the pathway could be overcome by means of synthase/reductase co-recruitment. We tethered varying numbers of SH3 peptide ligands (0,1,3,6 or 12), separated by flexible glycine-serine linkers, to the C terminus of HMGS and co-expressed these fusions either alone, or with HMGR bearing an N-terminal SH3 domain tag. Improvement in mevalonate production was seen for engineered co-recruitment of HMGS/R enzymes (**Fig. 2c**). As expected, this improvement depended on the presence of both the SH3 domain and the ligand, as well as the number of interactions.

Interestingly, mevalonate production reached an approximately tenfold maximum improvement with six possible interactions, which fell to sevenfold when the number of possible interactions was further increased. Three explanations are possible: (i) the increased local concentration effect from enzyme co-localization may be diminished with increasing number of ligands spatially separating the co-localized enzymes when the pool of HMGR is insufficient to saturate all of the binding sites, (ii) the limiting HMGR is sequestered such that it is unevenly distributed among the HMGS molecules, and/or (iii) addition of too many SH3 ligands leads to HMGS misfolding. Thus, mevalonate titers can be improved through both engineered co-localization of HMGS and HMGR as well as optimization of the number of introduced interaction ligands.

Separation of design control from catalytic activities

We next tested the scalability of the co-recruitment strategy by building separate scaffold devices capable of co-localizing multiple enzymes. Scaffolds provide a means for controlling design by physically separating catalytic activities from binding elements. Thus, the only modification to the enzyme necessary for gaining modular control over complex formation is the addition of a single interaction ligand to each enzyme. A peptide ligand specific for a corresponding protein-protein interaction domain was recombined to the C terminus of each enzyme of the mevalonate biosynthetic pathway (**Fig. 3a**). We built scaffolds by using flexible nine-residue glycine-serine linkers to tether, in various arrangements, three protein-protein interaction domains from metazoan genomes: the GTPase binding domain (GBD) from the actin polymerization switch N-WASP, the SH3 domain, and the PSD95/DlgA/Zo-1 (PDZ) domain from the adaptor protein syntrophin (**Supplementary Table 1**). Varying the number of repeats of these interaction domains provides control over the ratio of individual pathway enzymes co-localized to the resultant complex. Scaffolds were built with a single GBD domain for recruiting AtoB and varying numbers of SH3 and PDZ domains for recruiting HMGS and HMGR, respectively. The ability of the resultant scaffolds to bind each of the metabolic enzymes was confirmed using a GST-tagged version of a scaffold co-incubated with lysate containing each enzyme with the appropriate scaffold-targeting peptide ligand. The purified complex was digested with trypsin and the presence of each protein verified using mass spectrometry (**Supplementary Fig. 2**). Further, as expected, we did not observe any high-confidence peptides corresponding to non-scaffold targeted proteins, verifying the specificity of these eukaryotic interaction machineries in *E. coli* (data not shown).

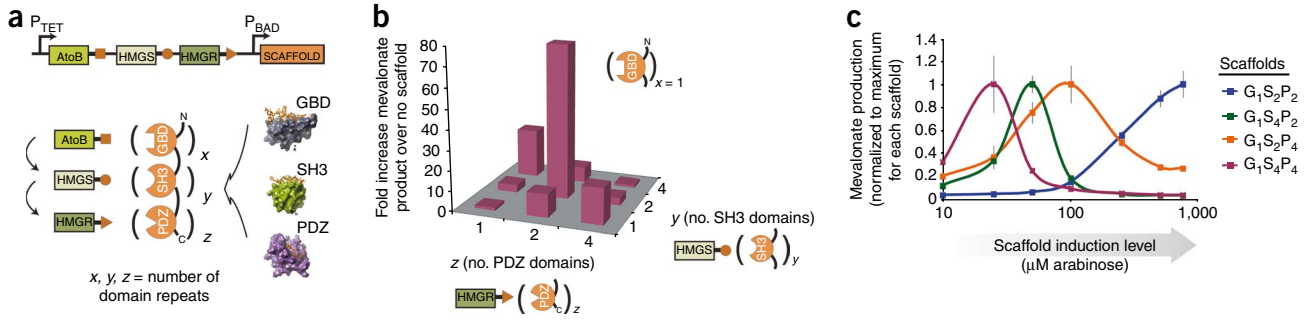

Figure 3 Synthetic scaffolds built from modular protein-protein interaction domains provide modular control over metabolic pathway flux. (**a**) The mevalonate pathway was placed under expression control of P_{TET}, and expression of the synthetic scaffolds was controlled by P_{BAD}. The synthetic scaffolds were constructed with three protein-protein interaction domains (GBD, SH3 and PDZ), where *x*, *y* and *z* represents the number of repeats of these domains, respectively. (**b**) A matrix of nine scaffolds exhibited dramatic differences in mevalonate product titers. Optimizing the relative number of recruitment domains ($GBD_1SH3_2PDZ_2$ or $G_1S_2P_2$) for maximum pathway flux resulted in a 77-fold increase in product titer compared to the non-scaffolded pathway ($G_0S_0P_0$). Improvements in mevalonate production levels were strongly dependent on scaffold architecture (**Supplementary Table 8**). (**c**) The scaffold induction level for optimal mevalonate production depends on the number of interaction domains. Scaffolds with higher numbers of interaction domain repeats ($G_1S_4P_4$) showed optimal mevalonate production at lower scaffold inducer concentrations than scaffolds with fewer domain repeats ($G_1S_2P_2$). Scaffolds with intermediate numbers of repeats ($G_1S_4P_2$ and $G_1S_2P_4$) showed optimal production at intermediate inducer concentrations. The lines connecting the points are not a fit and are meant only to highlight the data points for each scaffold. Raw data are plotted in **Supplementary Figure 8**.

A matrix of scaffolds was made with the architecture (N terminus to C terminus) of $GBD_xSH3_yPDZ_z$ where $x = 1$ and y and z were varied to be 1, 2 or 4. For separate inducible control, the pathway enzymes were placed under transcriptional control of P_{TET}, and the scaffolds were under transcriptional control of P_{BAD} (**Supplementary Fig. 1**). In an effort to lower the metabolic load imposed on the production host, mevalonate production experiments were conducted with low expression levels of the mevalonate pathway enzymes (7 nM aTc) and a high scaffold expression level (250 μM arabinose) to improve pathway efficiency.

Scaffolds improve product titers in a designable manner

Mevalonate titers were measured for the unscaffolded pathway ($GBD_0SH3_0PDZ_0$ or $G_0S_0P_0$), and improvements in production were plotted for each scaffold (**Fig. 3b**). A 77-fold increase in mevalonate production (titer of ~5 mM) was observed for the optimal scaffold ($G_1S_2P_2$). This scaffolding effect was observed as soon as mevalonate production was measureable (~12 h after inoculation) and persisted through to our final measurements (80 h after inoculation) (**Supplementary Fig. 3**). Production improvements depended on the number of interaction domain repeats in the scaffolds: varying the scaffold composition by a single domain often resulted in greater than an order-of-magnitude difference in mevalonate production. For example, scaffolds $G_1S_2P_2$ and $G_1S_1P_2$ differ by only one SH3 domain, yet produced dramatically different mevalonate titers: 77-fold versus fourfold, respectively. Further, scaffolds with differing numbers of interaction domain repeats varied in their flux-enhancing properties as the inducer was titrated to modulate scaffold expression (**Fig. 3c**). Scaffolds with higher numbers of domain repeats exhibited optimal mevalonate production at lower scaffold expression levels, whereas scaffolds with fewer domain repeats showed optimal mevalonate production at higher concentrations of inducer for scaffold expression. Scaffolds with intermediate numbers of interaction domains show optimal activities at intermediate expression levels. These results are consistent with the conclusions of others working with modeled scaffolded complexes, who observed an optimal concentration for any scaffold[26]. At high concentrations of scaffold, nonfunctional scaffold: enzyme stoichiometries can exist where the scaffold sequesters, rather than co-localizes, enzymes.

Role of scaffold architecture for improved product titers

We also investigated the role of domain orientation in scaffold architecture by rearranging the interaction domains of the optimized scaffold $G_1S_2P_2$ to $G_1S_1P_2S_1$ and $G_1S_1P_1S_1P_1$ (**Supplementary Fig. 4**). Compared to the optimal scaffold $G_1S_2P_2$ (77-fold improvement), scaffolds $G_1S_1P_2S_1$ and $G_1S_1P_1S_1P_1$ showed marked decreases in mevalonate production (tenfold and 22-fold higher titers than the unscaffolded pathway, respectively). Similarly, the effect of scaling the number of enzymes recruited to the scaffold was investigated by making scaffolds that recruited only HMGS and HMGR (**Supplementary Fig. 5**). As expected, enhancement of mevalonate biosynthesis was greater with scaffolds built to recruit all three enzymes than for those recruiting only HMGS/R (77-fold versus 8.5-fold). Thus, both the number of interaction domains targeting the enzymes to the scaffold and their orientation had dramatic impacts on their ability to increase pathway flux.

The role of scaffolding in flux enhancement was verified through a series of control experiments. First, a competing PDZ ligand was incorporated into the mevalonate pathway operon as a GST fusion and co-expressed with scaffold $G_1S_2P_2$ ($G_1S_2P_2$-competitor1; **Fig. 4a**). As expected, titers were lower using this construct than those resulting from the same construct lacking the competitive PDZ ligand ($G_1S_2P_2$). Mevalonate production was further decreased when the expression level of the GST-tagged PDZ ligand was increased by driving expression with P_{BAD} on a high copy plasmid ($G_1S_2P_2$-competitor2). Thus, an anomalous effect due to inducer or changing sequence was eliminated because inducer levels were held constant for all these experiments and the sequence of the plasmid containing the mevalonate biosynthetic enzymes was identical for $G_1S_2P_2$-competitor2 and $G_1S_2P_2$. Similarly, the effect of arabinose inducer for scaffold expression showed different effects depending on scaffold architecture. This is consistent with protein-complex stoichiometry determining product titers and not an anomalous effect of arabinose, independent of induction of scaffold expression (**Supplementary Fig. 8**). To verify that the scaffolding effect depends upon the peptide ligands recombined to each enzyme, we removed them ($G_1S_2P_2\Delta$ligands) and saw a dramatic decrease in mevalonate production compared to $G_1S_2P_2$. Recombining the peptide ligands to the pathway enzymes did seem to lower their collective activities somewhat, as $G_1S_2P_2\Delta$ligands

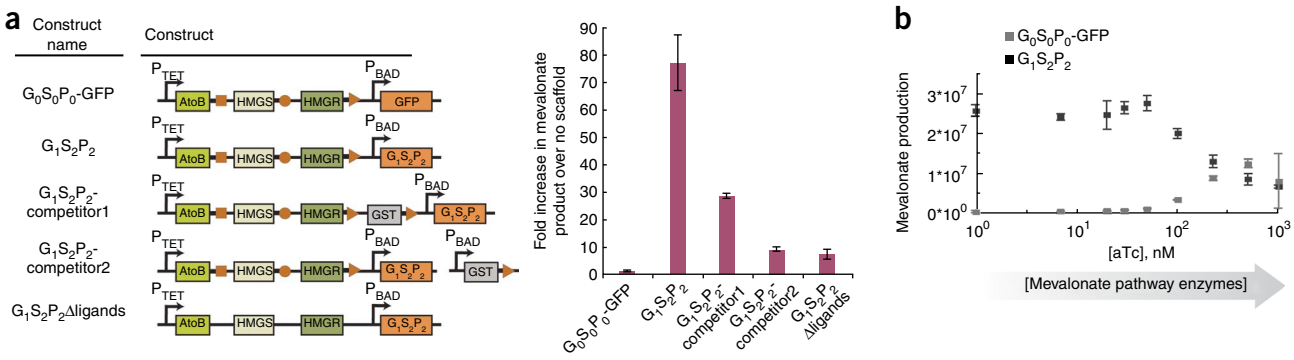

Figure 4 Enhancement of mevalonate production is scaffold-dependent. (**a**) Mevalonate production from the optimal scaffold $G_1S_2P_2$ was compared to that from control constructs ($G_0S_0P_0$-GFP, $G_1S_2P_2$-competitor1, $G_1S_2P_2$-competitor2, $G_1S_2P_2$Δligands). Expressing the green fluorescent protein ($G_0S_0P_0$-GFP) instead of a scaffold produced comparable mevalonate titers to expression of $G_0S_0P_0$. $G_1S_2P_2$-competitor1 was identical to $G_1S_2P_2$ with the exception of the addition of a competing PDZ ligand fused to a GST protein co-expressed as the last gene in the pathway operon. $G_1S_2P_2$-competitor1 produced less mevalonate than $G_1S_2P_2$, 29-fold versus 77-fold improvements over no scaffold, respectively. Increased expression of this competing PDZ ligand ($G_1S_2P_2$-competitor2) was achieved with a separate high copy plasmid (ColE1 origin) with P_{BAD} induced to saturation. The fold increase in mevalonate production over no scaffold was further decreased to ninefold. The necessity of the peptide tags recombined to the pathway enzymes was confirmed with construct $G_1S_2P_2$Δligands. (**b**) Use of synthetic scaffolds allows higher mevalonate titers to be achieved even with lower expression of pathway enzymes. High expression was achieved with an inducer concentration of 225 nM anhydrotetracycline, whereas low expression was achieved with 7 nM anhydrotetracycline. Error bars show 1 s.d. from an average of three separate experiments.

(without peptide ligands) produced ~7.5-fold higher mevalonate titers than $G_0S_0P_0$ or the control where instead of a scaffold, GFP was expressed ($G_0S_0P_0$-GFP). However, this loss of activity was more than compensated for by scaffolding ($G_1S_2P_2$). The ability to tag enzymes with interaction ligands without perturbing function will be protein-dependent and may require searching for accommodating locations for peptide insertions in other enzyme structures.

Lowered metabolic loads via increased pathway efficiency

A practical advantage of scaffolding is the improvement in pathway efficiency, allowing equivalent or higher titers to be achieved at lower enzyme expression levels than without the scaffold. Titers can be improved by directly mimicking substrate channeling, improving enzyme folding, reducing the propensity of enzymes to aggregate or a combination of these effects. Even at saturating inducer concentrations, the unscaffolded pathway ($G_0S_0P_0$) did not reach the mevalonate titers of the scaffolded pathway ($G_1S_2P_2$) obtained with basal expression levels (**Fig. 4b**). These scaffold-dependent increases in mevalonate production decreased as expression of pathway enzymes increased, suggesting that the concentration of scaffold was not sufficient to maintain function with high pathway enzyme concentrations. Growth curves indicate that much of the burden to the production host upon high induction of the mevalonate biosynthetic pathway can be relieved with expression of scaffold, achieving higher product titers with lower pathway enzyme expression (**Fig. 5**). In fact, additional expression of the scaffold on a co-transformed high-copy plasmid had minimal effects on growth rates but further increased mevalonate production. Similarly, cell cultures with the scaffolded pathway reached higher optical densities than those harboring the non-scaffolded pathway when pathway enzyme expression levels were low (**Supplementary Fig. 6**). However, this improvement in cell growth was not maintained when pathway enzyme expression was increased, consistent with our findings (**Fig. 4b**). Further support for the scaffold-dependent improvement in pathway efficiency is the observation that mevalonate production improved dramatically when the medium was supplemented with high concentrations of glycerol, but only when the pathway was scaffolded (**Supplementary Fig. 7**). Thus, scaffolds allowed the pathway to better use the increased carbon substrate, enabling higher product titers to be achieved with lower enzyme expression and decreasing the metabolic burden on the production host. Biotechnology applications—especially production of bulk compounds such as biofuels—require strategies that are orthogonal, yet compatible, to conventional methods to achieve commercially viable production levels. Improved pathway efficiency allowing lower enzyme expression may be particularly valuable for pathways containing enzymes that present a burden to express, have low solubilities or tendencies to aggregate.

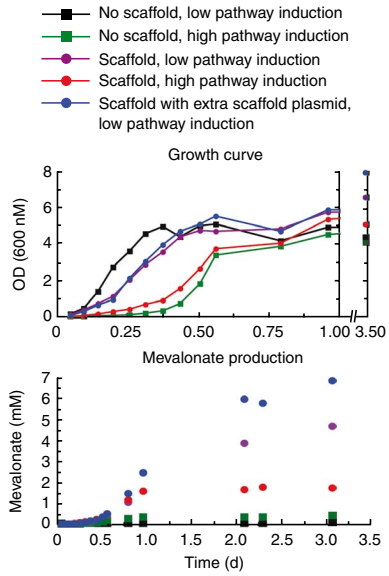

Figure 5 Improved efficiency from pathway scaffolding allows higher titers to be achieved with faster growth of the production host. High induction of the mevalonate biosynthetic pathway results from HMG-CoA accumulation[5]. Expression of scaffold ($G_1S_2P_2$) allows higher mevalonate to be produced at low pathway induction. At this low induction, the growth rate of *E. coli* is dramatically increased over strains with the pathway highly induced. A high-copy plasmid expressing additional scaffold ($G_1S_2P_2$) did not hinder growth, but further improved titer.

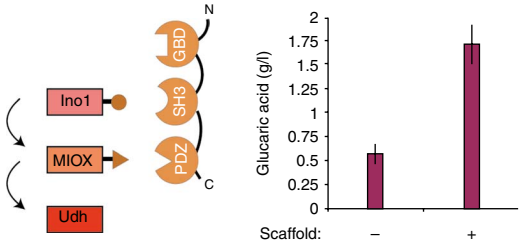

Figure 6 Improvement of glucaric acid titers by scaffolding the bottleneck step enzymes Ino1 and MIOX. Despite high initial titers of 0.5 g/l, scaffolded co-recruitment of Ino1 and MIOX with $G_1S_1P_1$ increased yields 200%.

Modular design of scaffolds is generalizeable

We applied the scaffolding strategy to the synthetic pathway for glucaric acid, a potential building block for several polymers, including new nylons and hyper-branched polyesters[27]. Biological routes to synthesis may provide higher yield and chiral selectivity than the currently used nonselective, expensive chemical process using nitric acid as the oxidant[27]. High titers of glucaric acid are generated by a pathway comprising three enzymes from three different organism sources, heterologously expressed using a T7 promoter system in *E. coli*[28]. Despite this high yield, we further improved product titers by scaffolding the two enzymes representing the bottleneck step, *myo*-inositol-1-phosphate synthase (Ino1) and *myo*-inositol oxygenase (MIOX), despite employing the lower expression P_{lac} system. Product titers were improved 200% over a non-scaffolded control to produce a maximum titer of 1.7 g/l (**Fig. 6**). Thus, we were able to reuse a scaffold for a pathway completely orthogonal to the mevalonate biosynthetic pathway. Additional gains may be achievable by testing the entire matrix of scaffolds described here, as well as designing others as needed. Considering the high initial titers, this improvement is impressive and represents the type of gains needed in the biotechnology field, especially for production of bulk compounds, to achieve viable yields. Notably, we were able to apply the scaffolding strategy in a complementary manner to more conventional strategies such as optimization of pathway enzyme expression levels.

DISCUSSION

We exploited the naturally evolved modularity of protein-protein interaction domains to facilitate the rapid design and optimization of flux-increasing scaffolds. This strategy was inspired by natural biosynthetic machines (e.g., polyketide synthases, fatty acid synthases and non-ribosomal peptide synthases) that produce small molecules by channeling intermediates iteratively through assembly lines of catalytic activities. Although simpler than these elegant natural systems, the modular design of our scaffold strategy should prove to be both programmable and generalizeable. Scaffolding might complement conventional strategies for balancing enzymatic activities for achieving increased product levels. The modular scaffold design facilitated the rapid optimization of pathway flux through control over the stoichiometry of enzymes recruited to the functional complex. As this design does not depend on structural characteristics of an enzyme, other than the ability to tether a short peptide ligand without perturbing activity, it should prove to be generalizeable to other pathways.

The widely appreciated importance of modularity in evolution, as well as its efficacy for engineering behaviors, is especially clear for transcriptional networks where the output coding sequence to be expressed is physically and functionally separable from its *cis*-regulating element (promoter). Synthetic biologists have taken advantage of this modularity to build genetic circuits with targeted behaviors such as 'the repressilator' and toggle switch[29,30]. Similarly, modularity in many protein designs has recently been used to forward-engineer biological systems with desired behaviors[25,31–33]. Engineered metabolic pathways are one type of biological system where introduction of flux control through protein-design can produce quantifiable improvements in product titers. Scaffolding offers an orthogonal, but complementary, strategy to conventional approaches such as transcriptional control of enzyme expression and enzyme optimization through directed evolution. Increased designable control of these complex biological systems will be required to achieve product titers adequate to meet demands for products such as therapeutics and biofuels. Synthetic scaffolds should provide engineerable nodes for introducing this modular control and promises to provide a platform for additional synthetic biology applications.

METHODS

Methods and any associated references are available in the online version of the paper at http://www.nature.com/naturebiotechnology/.

Note: Supplementary information is available on the Nature Biotechnology website.

ACKNOWLEDGMENTS

We thank A. Arkin, J. Dietrich, E. Dueber, L. Katz, and W. Whitaker for comments and discussion during the preparation of the manuscript. We also thank members of the Dueber and Keasling labs for experimental help and discussions. This work was supported by funding from UC Berkeley QB3 Institute (J.E.D.), National Science Foundation (NSF) Synthetic Biology Engineering Research Center grant no. EEC-0540879 (J.E.D., J.D.K, K.L.J.P., T.S.M.), NSF grant no. CBET-0756801 (J.E.D.), the Bill and Melinda Gates Foundation (J.D.K), Joint BioEnergy Institute (J.D.K.), the Office of Naval Research Young Investigator Program grant no. N000140510656 (K.L.J.P. and T.S.M.).

AUTHOR CONTRIBUTIONS

J.E.D. conceived the project, designed all experiments and wrote the manuscript. J.E.D. and G.C.W. co-performed the experiments, and G.C.W. edited the manuscript. G.R.M. constructed and performed preliminary experiments used as a foundation for experiments included in this paper. T.S.M. contributed an experimental role for glucaric acid pathway experiments and edited the manuscript. C.J.P. contributed an experimental role for mass spectrometry experiments. A.V.U. contributed a supportive role in performing experiments for Supplementary Information Materials. K.L.J.P. contributed in development of the glucaric acid pathway and edited the manuscript. J.D.K. contributed general advice, especially with the mevalonate biosynthesis pathway, resource support and critical advice for manuscript preparation.

COMPETING INTERESTS STATEMENT

The authors declare competing financial interests: details accompany the full-text HTML version of the paper at http://www.nature.com/naturebiotechnology/.

Published online at http://www.nature.com/naturebiotechnology/.
Reprints and permissions information is available online at http://npg.nature.com/reprintsandpermissions/.

1. Stephanopoulos, G. Challenges in engineering microbes for biofuels production. *Science* **315**, 801–804 (2007).
2. Nakamura, C.E. & Whited, G.M. Metabolic engineering for the microbial production of 1,3-propanediol. *Curr. Opin. Biotechnol.* **14**, 454–459 (2003).
3. Khosla, C. & Keasling, J.D. Metabolic engineering for drug discovery and development. *Nat. Rev. Drug Discov.* **2**, 1019–1025 (2003).
4. Harcum, S.W. & Bentley, W.E. Heat-shock and stringent responses have overlapping protease activity in *Escherichia coli*. Implications for heterologous protein yield. *Appl. Biochem. Biotechnol.* **80**, 23–37 (1999).
5. Kizer, L., Pitera, D.J., Pfleger, B. & Keasling, J.D. Functional genomics for pathway optimization: application to isoprenoid production. *Appl. Environ. Microbiol* **74**, 3229–3241 (2008).
6. Zhu, M.M., Lawman, P.D. & Cameron, D.C. Improving 1,3-propanediol production from glycerol in a metabolically engineered *Escherichia coli* by reducing accumulation of sn-glycerol-3-phosphate. *Biotechnol. Prog.* **18**, 694–699 (2002).
7. Barbirato, F., Grivet, J.P., Soucaille, P. & Bories, A. 3-Hydroxypropionaldehyde, an inhibitory metabolite of glycerol fermentation to 1,3-propanediol by enterobacterial species. *Appl. Environ. Microbiol.* **62**, 1448–1451 (1996).

8. Stephanopoulos, G. Metabolic fluxes and metabolic engineering. *Metab. Eng.* **1**, 1–11 (1999).
9. Pitera, D.J., Paddon, C.J., Newman, J.D. & Keasling, J.D. Balancing a heterologous mevalonate pathway for improved isoprenoid production in. *Escherichia coli. Metab. Eng.* **9**, 193–207 (2007).
10. Pfleger, B.F., Pitera, D.J., Smolke, C.D. & Keasling, J.D. Combinatorial engineering of intergenic regions in operons tunes expression of multiple genes. *Nat. Biotechnol.* **24**, 1027–1032 (2006).
11. Bloom, J.D. *et al.* Evolving strategies for enzyme engineering. *Curr. Opin. Struct. Biol.* **15**, 447–452 (2005).
12. Miles, E.W., Rhee, S. & Davies, D.R. The molecular basis of substrate channeling. *J. Biol. Chem.* **274**, 12193–12196 (1999).
13. Spivey, H.O. & Ovadi, J. Substrate channeling. *Methods* **19**, 306–321 (1999).
14. Hyde, C.C., Ahmed, S.A., Padlan, E.A., Miles, E.W. & Davies, D.R. Three-dimensional structure of the tryptophan synthase alpha 2 beta 2 multienzyme complex from Salmonella typhimurium. *J. Biol. Chem.* **263**, 17857–17871 (1988).
15. Thoden, J.B., Holden, H.M., Wesenberg, G., Raushel, F.M. & Rayment, I. Structure of carbamoyl phosphate synthetase: a journey of 96 A from substrate to product. *Biochemistry* **36**, 6305–6316 (1997).
16. Conrado, R.J., Varner, J.D. & DeLisa, M.P. Engineering the spatial organization of metabolic enzymes: mimicking nature's synergy. *Curr. Opin. Biotechnol.* **19**, 492–499 (2008).
17. Mosbach, K. & Mattiasson, B. Matrix-bound enzymes. II. Studies on a matrix-bound two-enzyme-system. *Acta Chem. Scand.* **24**, 2093–2100 (1970).
18. Bulow, L. Characterization of an artificial bifunctional enzyme, beta-galactosidase/galactokinase, prepared by gene fusion. *Eur. J. Biochem.* **163**, 443–448 (1987).
19. Bulow, L., Ljungcrantz, P. & Mosbach, K. Preparation of a soluble biofunctional enzyme by gene fusion. *Bio/Technology* **3**, 821–823 (1985).
20. Martin, V.J., Pitera, D.J., Withers, S.T., Newman, J.D. & Keasling, J.D. Engineering a mevalonate pathway in *Escherichia coli* for production of terpenoids. *Nat. Biotechnol.* **21**, 796–802 (2003).
21. Nagar, B. *et al.* Structural basis for the autoinhibition of c-Abl tyrosine kinase. *Cell* **112**, 859–871 (2003).
22. Prehoda, K.E., Scott, J.A., Mullins, R.D. & Lim, W.A. Integration of multiple signals through cooperative regulation of the N-WASP-Arp2/3 complex. *Science* **290**, 801–806 (2000).
23. Dueber, J.E., Yeh, B.J., Bhattacharyya, R.P. & Lim, W.A. Rewiring cell signaling: the logic and plasticity of eukaryotic protein circuitry. *Curr. Opin. Struct. Biol.* **14**, 690–699 (2004).
24. Dueber, J.E., Yeh, B.J., Chak, K. & Lim, W.A. Reprogramming control of an allosteric signaling switch through modular recombination. *Science* **301**, 1904–1908 (2003).
25. Dueber, J.E., Mirsky, E.A. & Lim, W.A. Engineering synthetic signaling proteins with ultrasensitive input/output control. *Nat. Biotechnol.* **25**, 660–662 (2007).
26. Levchenko, A., Bruck, J. & Sternberg, P.W. Scaffold proteins may biphasically affect the levels of mitogen-activated protein kinase signaling and reduce its threshold properties. *Proc. Natl. Acad. Sci. USA* **97**, 5818–5823 (2000).
27. Werpy, T. & Petersen, G. Top value added chemicals from biomass. vol. I: Results of screening for potential candidates from sugars and synthesis gas (US Dept. of Energy, Oak Ridge, Tennessee and Dept. of Commerce, Springfield, Virginia; 2004). ⟨http://www.pnl.gov/main/publications/external/technical_reports/PNNL-14808.pdf⟩.
28. Moon, T.S., Yoon, S.H., Lanza, A.M., Roy-Mayhew, J.D. & Prather, K.L. Production of glucaric acid from a synthetic pathway in recombinant *Escherichia coli*. *Appl. Environ. Microbiol.* **75**, 589–595 (2009).
29. Elowitz, M.B. & Leibler, S. A synthetic oscillatory network of transcriptional regulators. *Nature* **403**, 335–338 (2000).
30. Gardner, T.S., Cantor, C.R. & Collins, J.J. Construction of a genetic toggle switch in *Escherichia coli*. *Nature* **403**, 339–342 (2000).
31. Bashor, C.J., Helman, N.C., Yan, S. & Lim, W.A. Using engineered scaffold interactions to reshape MAP kinase pathway signaling dynamics. *Science* **319**, 1539–1543 (2008).
32. Howard, P.L., Chia, M.C., Del Rizzo, S., Liu, F.F. & Pawson, T. Redirecting tyrosine kinase signaling to an apoptotic caspase pathway through chimeric adaptor proteins. *Proc. Natl. Acad. Sci. USA* **100**, 11267–11272 (2003).
33. Yeh, B.J., Rutigliano, R.J., Deb, A., Bar-Sagi, D. & Lim, W.A. Rewiring cellular morphology pathways with synthetic guanine nucleotide exchange factors. *Nature* **447**, 596–600 (2007).

ONLINE METHODS

Mevalonate biosynthesis pathway. A plasmid encoding the mevalonate pathway enzymes, codon optimized for expression in *E. coli*, (MevT66) was amplified by multistep PCR using primers that incorporated unique restriction enzyme sites between the pathway enzymes. These unique restriction enzyme sites were used to insert sequences encoding the peptide ligands and poly-GLY-SER linkers connecting the enzyme to these ligands. Oligonucleotides (Integrated DNA Technologies) encoding these ligands were phosphorylated separately by incubation with T4 polynucleotide kinase (New England Biosciences) for 60 min at 37 °C (1 µl of a 100 µM stock in a total volume of 10 µl). The phosphorylated oligonucleotides were pooled in a total volume of 100 µl, placed in a beaker of boiling water for 5 min, and left in the water bath with the heat source removed until it reached ambient temperature. The inserts were designed to have cohesive ends compatible with digested vector when properly annealed. 3 µl was used as insert for a ligation reaction with the appropriate digested vector. The ligation products were transformed into KCM (KCl, CaCl2, MgCl2) chemical competent DH10B *E. coli* cells.

Construction of HMGS/HMGR direct corecruitment constructs. The pZB plasmid with two independent promoters, the arabinose-inducible P_{BAD} and the tetracycline-inducible P_{TET}, was used[34]. An SH3 domain (from the mouse protein Crk, residues 134–191) was attached via a nine-residue poly-glycine-serine linker to the N terminus of HMGR using multistep PCR and inserted behind P_{TET} by ligation of compatible cohesive ends created by the restriction enzymes PstI and NheI to create pZB001. As a control, HMGR alone was PCR amplified and inserted behind the P_{TET} by ligation of compatible cohesive ends created by the restriction enzymes PstI and NheI to create pZB003. These two plasmids were used as parental vectors that could be digested with the restriction enzymes SphI and NotI and accept SphI/NotI digested inserts containing AtoB and HMGS with a variable number of SH3-binding motifs previously constructed.

One and three peptide containing constructs, with poly-GLY-SER linkers N-terminal to each linker, were made with multiple oligonucleotides as described above. Six-peptide repeats were constructed by PCR amplifying the three-peptide repeat construct with primers that added an XbaI site downstream of the 5′ XhoI site and a 3′ SpeI site upstream of the 3′ ApaI site. XbaI and SpeI digestion products are compatible for ligation. Half of the product was digested with XbaI, whereas the other half was digested with SpeI. The resultant products were ligated, the desired size gel purified, digested with XhoI and ApaI, and ligated into XhoI/ApaI-digested vector. A similar strategy was used to make the 12-peptide repeat construct using the six-peptide repeat as the digested substrate for SpeI/XbaI ligation.

Construction of synthetic scaffolds. Scaffolds were built by tethering multiple protein-protein interaction domains via nine-amino acid poly-GLY-SER linkers using the BioBrick b (BBb) strategy[35]. Basic parts consisting of a DNA sequence encoding the N-terminal linker and the interaction domain were made with 5′ flanking EcoRI/BglII restriction enzyme sites and 3′ BamHI/XhoI restriction enzyme sites. These basic parts were combined in desired arrangements by digesting the ultimate upstream part with BamHI and XhoI and the downstream part with BglII and XhoI and ligating. The cohesive ends created by BamHI and BglII are compatible for ligation and destroy both of these recognition sites. Thus, the resultant composite part maintains the original unique restriction enzyme pattern for further addition of other parts. In this manner synthetic scaffolds were constructed by iterative addition of parts.

GST pull-down: protein construction, expression and pull-down. Proteins were expressed as fusions to either a cleavable hexa-histidine tag (pET19-derived vector)[36] or glutathione S-transferase (GST) (pGEX4T, Pharmacia) in *E. coli* (BLR-DE3) as previously described[25]. Overnight cultures were inoculated to an optical density (OD) of 0.05 in 500 ml of Luria Bertani broth (LB). The cultures were grown at 30 °C to an OD of 0.5–0.75 and induced with 0.5 mM isopropyl-beta-D-thiogalactopyranoside (IPTG) for 5 h. The cultures were pelleted by centrifugation and resuspended in 35 ml of PBS supplemented with 2 mM dithiothreitol (DTT). Cells were lysed by sonication (VirSonic) and centrifuged. The soluble fraction was decanted, aliquoted and flash-frozen in liquid nitrogen until the pull-down experiments were conducted.

GST-fusion binding assays were performed by immobilizing GST-fusion proteins on glutathione agarose beads (Sigma). A 50% slurry of glutathione agarose beads was made in PBS supplemented with 2 mM DTT. 50 µl of this 50% slurry to one 1.5 ml aliquot of GST-tagged construct lysate and incubated at 4 °C for 15 min with frequent rotation. Glutathione agarose beads were pelleted by a low-speed spin on a Galaxi Minicentrifuge (VWR). The supernatant was aspirated and the beads washed three times with PBS supplemented with 2 mM DTT. After the third wash, the beads were left as a 50% slurry in PBS supplemented with 2 mM DTT. 20 µL of the resultant bead slurry was combined with a 1.5 ml aliquot of prey lysate of HMGR with or without an N-terminal SH3 domain and incubated at 4 °C for 15 min with rotation. Four 1.5 ml washes were performed with PBS supplemented with 2 mM DTT and 0.05% Tween-20. After the last aspiration, 20 µl of 2× SDS buffer was added and run on a NuPAGE Novex 4–12% Bis-Tris Gel (Invitrogen) and stained with Coomassie.

Mevalonate pathway expression/mevalonate production. The mevalonate pathway with scaffold was cloned as described above in the *E. coli* strain DH10B. Pathway expression experiments were conducted in *E. coli* DP10 cells, a strain built and previously described[20]. Briefly, this strain contains a chromosomal copy of *araE* constitutively expressed by the PCP8 promoter and combined with a deletion of *araFGH* as described[37]. Thus DP10 cells exhibit a linear response in expression of genes under control of P_{BAD} as a function of arabinose concentration across the population. Starting cultures were grown in LB broth and then diluted in 5 ml LB broth supplemented with 4% glycerol, 34 µg/ml chloramphenicol, and the desired concentration of arabinose and anhydrotetracycline (aTc) inducers such that the final OD_{600} was 0.05. The cells were then grown in 25-mm culture tubes for 50 h at 37 °C with shaking at 200 r.p.m. in the dark after which mevalonate was acidified and extracted with ethyl acetate, as detailed below.

Mevalonate extraction/GC-MS analysis. Mevalonate abundance was determined by acidifying cell cultures to form mevalonolactone followed by extraction with ethyl acetate. After 50 h of expression, 140 µl 0.5 M HCl was added to 560 µl *E. coli* culture and then vortexed for 45 s, which converts mevalonate to mevalonolactone. Extractions were performed by addition of 700 µl ethyl acetate supplemented with 4.5–5.0 µg/ml of the internal standard caryophyllene. The samples were then vortexed for 5 min using the highest setting and then spun down for 3 min at 2,080 r.c.f. using Eppendorf centrifuge model 5417C. After centrifugation, 400 µl of the top layer was added to 200 µl ethyl acetate and 4.5–5.0 µg/ml caryophyllene. The sample was then run on Agilent Technologies chiral cyclosil-B column (30 m length × 0.25 mm i.d. × 0.25 µm Film). Helium was used as the carrier gas at a constant flow of 1 ml/min and 1 µl spit-less injections were performed. The injection port was maintained at 250 °C, the MS source temperature was maintained at 230 °C, and the MS quad temperature was held constant at 150 °C. The column temperature profile was 90 °C for 1 min; 30 °C/min to 250 °C and held at 250 °C for 2 min. The selected ions monitored were *m/z* 71 and 58 for mevalonic acid lactone, and *m/z* 189 and 204 for (–)-trans-caryophyllene. Retention time, mass spectrum and concentration of extracted mevalonic acid lactone were confirmed using DL-mevalonic acid lactone (Sigma). Chromatograms were analyzed using Agilent MSD Productivity ChemStation for GC and GC/MS Systems Data Analysis Application. Retention times for mevalonolactone were determined by comparing to a mevalonolactone standard. Agilent GC/MS software was used to integrate the area under the peaks to determine the relative abundance of mevalonolactone and, therefore, mevalonate abundance in the samples.

Complex analysis of scaffold/enzyme complex by GST-pull-down and mass spectrometry. Scaffold $G_1S_1P_1$ and $G_1S_2P_2$ were N-terminally GST tagged and pull-downs were conducted as described above. Samples were run on a NuPAGE 4–12% Bis-Tris Gel 1.0 mm × 17 well (Invitrogen), and entire gel lanes were cut and used for in-gel trypsin digestion following the protocol as described[38]. Peptide samples were analyzed on a LC-MS/MS system consisting of an Eksigent TEMPO nanoLC-2D coupled to an Applied Biosystems 4000Q-Trap mass spectrometer operating in multiple reaction monitoring (MRM) mode. The peptide samples were loaded onto a Pepmap100 µ-guard column

doi:10.1038/nbt.1557

(Dionex-LC Packings) via a Famos Autosampler (Dionex-LC Packings) and were washed for 30 min (15 µl/min flow rate) before injection onto a Dionex Pepmap100 analytical column (75 µm I.d., 150 mm length, 100Å, 3 µm) at a flow rate of 300 nl/min using buffers 98% H_2O, 2% acetonitrile, 0.1% formic acid (A) and 98% acetonitrile, 2% H_2O, 0.1% formic acid (B). The LC gradient was as follows: 0–35% B over 90 min, 35–80% B in 10 min. The solvent composition was held at 80% B for 10 min followed by a short ramp back to 100% A and a re-equilibration period at 100% A for 15 min.

Data were collected with Analyst 1.5 (Applied Biosystems) operating in information dependent acquisition (IDA) mode and consisting of a MRM survey scan and one product ion (MS/MS) scan. MRM transitions were generated from nontargeted IDA LC-MS/MS runs of digests of the proteins of interest (scaffold, AtoB, HMGS, HMGR). The IDA mode was triggered for MRM transitions of >1,000 counts/s to verify that the correct peptide signal is detected. MS/MS spectra were collected for 2 s over a mass range of 100–1,600 *m*/*z* with Q1 resolution = LOW and rolling collision energy.

Construction of glucaric acid pathway. The pathway was cloned as described[28] with the peptide ligands recognizing the scaffold added by multistep PCR. The scaffold was subcloned into the expression plasmid such that it was downstream of Ino1 and MIOX in the same operon. Udh, amplified from *P. syringae* genomic DNA was cloned into the expression vector pSTV28 with SmaI behind P_{lac}. BL21 Star (DE3) (Invitrogen) expression strains were made by co-transforming the plasmid driving Ino1, MIOX and scaffold expression in a single operon and the plasmid driving expression of Udh—both by the P_{lac}.

Culture and analysis conditions for D-glucaric acid production. Cultures were grown in LB medium supplemented with 10 g/l D-glucose and induced at the exponential phase with 0.2 mM IPTG. An inoculum was prepared in LB medium, and 1% (vol/vol) was used to inoculate 250-ml baffled flasks containing 50 ml of medium. The cultures were incubated at 30 °C and 250 r.p.m. for 2 d, and then D-glucaric acid titer was analyzed using HPLC as described previously[28].

34. Lee, S.K., Newman, J.D. & Keasling, J.D. Catabolite repression of the propionate catabolic genes in *Escherichia coli* and *Salmonella enterica*: evidence for involvement of the cyclic AMP receptor protein. *J. Bacteriol.* **187**, 2793–2800 (2005).
35. Shetty, R.P., Endy, D. & Knight, T.F. Jr. Engineering BioBrick vectors from BioBrick parts. *J. Biol. Eng.* **2**, 5 (2008).
36. Hillier, B.J., Christopherson, K.S., Prehoda, K.E., Bredt, D.S. & Lim, W.A. Unexpected modes of PDZ domain scaffolding revealed by structure of nNOS-syntrophin complex. *Science* **284**, 812–815 (1999).
37. Khlebnikov, A., Datsenko, K.A., Skaug, T., Wanner, B.L. & Keasling, J.D. Homogeneous expression of the P(BAD) promoter in *Escherichia coli* by constitutive expression of the low-affinity high-capacity AraE transporter. *Microbiology* **147**, 3241–3247 (2001).
38. Shevchenko, A., Tomas, H., Havlis, J., Olsen, J.V. & Mann, M. In-gel digestion for mass spectrometric characterization of proteins and proteomes. *Nat. Protocols* **1**, 2856–2860 (2006).